Eighth International Conference on
THIN-WALLED STRUCTURES – ICTWS 2018
Lisbon, Portugal, July 24-27, 2018

COMPUTATIONAL GRID GENERATION ON THE DESIGN OF FREE-FORM SHELLS WITH COMPLEX BOUNDARY CONDITIONS

Jun Ye[*,*], Tierui Li[**], Paul Shepherd[*] and Boqing Gao[**,***]**

* Department of Architecture and Civil Engineering, University of Bath, Bath, UK

j.ye@bath.ac.uk

** College of Civil Engineering and Architecture, Zhejiang University, Hangzhou, China

*** Zhejiang Provincial Key Laboratory of Space Structures, Hangzhou, China

Keywords: Free-form grid shell; Complex boundary; Surface flattening; Guide line method; Grid generation; Grid relaxation

Abstract. *The free-form grid structures have been widely used in various public buildings, and many of them are trimmed with complex curves including internal voids. Computational design software enables the rapid conceptual creation of such complex surface geometry, whereas it is neither a convenient nor an obvious task for engineers to create a discrete grid structure on a free-form surface with complex boundary conditions that manifest the designer's intension. This emphasizes the importance of grid generation tools and methods in the initial design stage. This paper presents an efficient design tool for the synthesis of free-form grid structures based on the "guide line" and surface flattening methods, considering complex features of internal boundaries on trimmed free-form surface. The method employs a fast and straightforward approach which achieves grids with rods of balanced length and fluent lines. In order to generate grids on the trimmed free-form surface with complex boundaries, the grid generation method which combines surface flattening and improved guide line method is put forward. The data of trimmed surface includes a complete surface and the trimming curves. The parametric domain of the complete NURBS surface was firstly divided into a number of parts and a discrete free-form surface was accordingly formed by mapping dividing points onto surface. The free-form surface was then flattened based on the principle of identical area. Accordingly, the flattened rectangular lattices were fitted into the 2D surface where grids were formed applying the guide line method. Subsequently, the intersections of guide lines and the complex boundary were obtained and the guide lines were modified and divided equally to get grids by connecting dividing points. Finally, the 2D grids were mapped onto the 3D surface to achieve grid on free-form surface with complex boundaries. A spring-mass method was also employed to further improve the smoothness of the resulted grids. Examples were presented to shown the effectiveness of the proposed method.*

1 INTRODUCTION

Grid shells as long spanning roof structures, is often the most striking part in a building from a designer's perspective. Grid shells provide a sense of simplicity and elegance in terms of appearance. The important features of grid shells are their appeal of uninterrupted span, the smoothness of their continuum surface counterparts, the lightness of their grid cells, curve fluidity and most importantly their high structural efficiency that can resist external actions through membrane stiffness [1]. Grid shells with plane, cylinder, sphere, and parabolic shapes [2-4] have been widely used in engineering practice, where engineers easily use analytical equations to generate nodal positions and members for grid structural design use.

Free-form surface, however, is unable to be expressed accurately by means of several analytic functions and the curvature of such a surface is generally complex, as shown in Fig.1. In recent years, parametric modeling and scripting techniques in computer aided design have enabled a new level of sophistication in 3D free-form surface, allowing engineers searching for techniques to restructure the design process and inspire their imagination further. The aesthetically pleasing nature-designs also attract the attention from the construction market for new buildings. The number of new and complex free-form grid structures on complex curved surface is therefore increasing. Given the varying curvature and complex boundaries, it is a tedious job for designers to generate grid on a curved free-form surface, despite the fact that the advancement of CAD technology has allowed for freedom to control the architectural form.

Figure 1: Free-form grid structures: the British Museum Great Court.

The grid pattern of free-form grid shells are traditionally created by hand using computer-aided design tools or automated by using tailored scripts for each individual project. As the free-form grid structures are becoming more popular and complex, a practical grid generation tool which can efficiently generate a structural grid on a given free-form surface is becoming more necessary to facilitate the design process, particularly in the early design stage. A highly efficient grid generation method for the design of free-form grid shells is distinct in 4 aspects: (1) Grids generated should be an approximation to the given surface; (2) as equal rod length of each member as possible for the ease of manufacturing and connecting, as shown in Fig. 2; (3) fluidity of each curve embedded into the surface to seed the general orientation of pattern (Fig.2) and (4) a standard tool for the automation of grid generation and fast evaluation on complex surfaces.

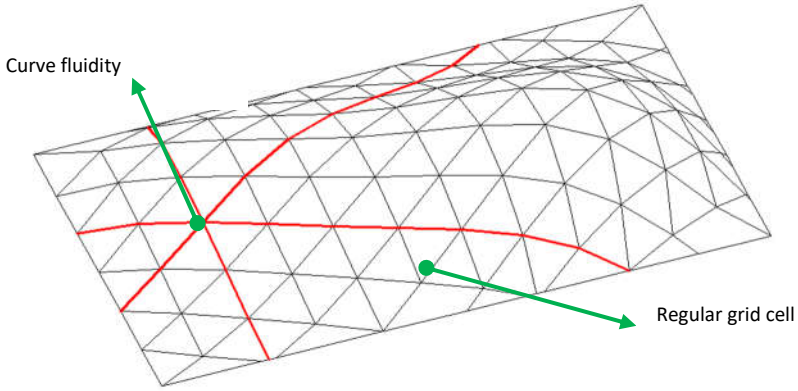

Figure 2: Grid shell with curve fluidity and regular grid cells.

Traditional mesh generation methods have been developed and applied to finite-element analysis, with the mainstream and standard methods such as Advancing Front Technique [5], Mapping Method [6] and Delaunay Triangulation [7, 8]. These methods can be adapted for the gird generation for the design of shells, whereas the resulted topology does not necessarily meet the requirement of equal rod length and the architectural grid fluidity.

Grid generation methodologies on free-form surface are attracting researchers' attention whilst the research is rather limited. Early method for the grid generation on a 3D surface is known as Chebyshev net design proposed in 1878 [9]. Two arbitrary intersecting curves were first defined on the given surface; each curve was then divided into segments with the same rod length. The rest of points was then produced by using the intersection between 2 adjacent circles on the surface with each circle has a radius of the same rod length. Due to the use of 3D circles over the surface, this method is more specific as "Compass Method", as shown in Fig.3. Lefevre et al. [10] used the "Compass Method" to generate grid shell for instability analysis while a method with denser Chebyshev net was proposed to improve the quality of resulted grid. Shepherd and Richens [11] proposed the Subdivision Surface method, where an initial triangular or quadrilateral mesh is first imposed onto a free-form surface and then subdivided over a number of iterations and fit the original surface. More recently, Douthe et al. [12] proposed a method to generate the shape of grid shells covering with quadrilateral grid cells. Using two intersection curves as guide lines, a circular mesh was generated, the duality between a circular mesh with a unique radius and Tchebycheff net was used to obtain quadrilateral grid. In their method of grid generation, the planarity of each grid cell has been taken into account.

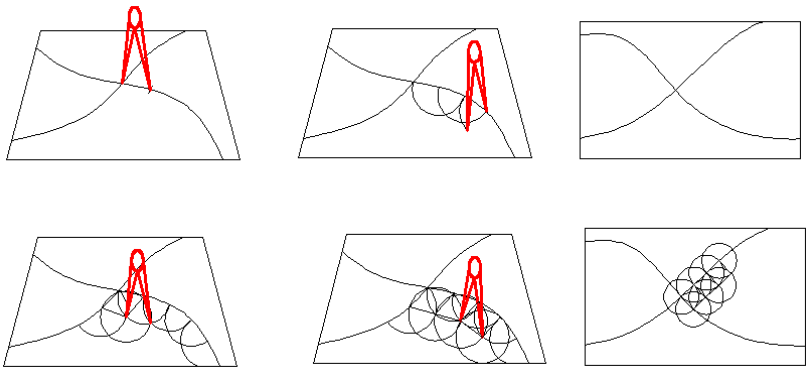

Figure 3: Compass method.

Recently, Gao et al. [13] proposed a "guide line method" for the synthesis of free-form grid structures. The method is straightforward and is able to obtain grids with rods of balanced length and fluent lines. The process started with defining a limited number of curves (named the guide lines) on the surface, the guide lines were then advanced over the surface which were then used to determine the directions of the 'rods' of the grid. It was shown that the generated grids were generally with approximate rod length and fluidity. Gao et al. [14] proposed a more advanced grid generation method that combined a surface flattening technique with the guide line method. Dividing points were firstly generated on the parametric domain and were then mapped to the free-form surface. Using a principle of identity area, the surface was then flattened and grids were generated by advancing the guide line on the flattened surface. The resulted grids were finally mapped back onto the surface and a quality index was used to evaluate the regularity of grid cells. It was found that the grid

shape quality index and the deviation of rod length of the grid structure were reduced by up to 47%, with and without using the surface flattening technique.

In practice, the free-form surfaces of grid shells are more complex with trimmed boundary conditions. The free-form surface is usually trimmed by a curve or a sub-surface so that the free-form surface with complex boundary is obtained. Cases are presented in Fig.4, where the free-form surface is with internal boundaries, which is trimmed by one or several closed space curves. The available research on grid generation was generally conducted for the development of grid generation on complete free-form surface, while there is no emphasis on the grid generation method that considering complex boundary conditions for the design of free-form grid shells.

Figure 4: Free-form grid structures with complex boundaries: Shenzhen Bay Sports Center.

Compared to previous studies, the main development of this paper is to take into account the complex boundary conditions for grid generation on a given free-form surface, by combining surface flattening technique with improved guide line method. Using the guide line method to generate grids on a surface, the fluidity is guaranteed by an input curve that manifests the designer's intention for the direction of grids and defines initial seed features to control the final results. 3D free-form surface can be flattened into a 2D plane by using a surface flattening technique, which facilitates the guide line advancing process. The intersection points are therefore calculated by using the intersection of resulted guide lines and the given complex boundary curves. Members of structural geometry which are outside the design domain will then be deleted. This paper also optimises the smoothness of the resulted grids by using a spring-mass method. A grid pattern that satisfy the requirement of equal rod length and fluidity will be obtained and more importantly, the resulted grid pattern will be strictly compatible to the given irregular boundary conditions, which has not been highlighted in previous research.

2 DESCRIPTIONS OF CURVES AND SURFACES

NURBS (Non-uniform rational B-Splines) expressions [15] are used in this paper to represent the free-form surface. NURBS has been the industry standard that is used for shape representation, design and data exchange when geometric information is processed by computer. As a result, NURBS is a powerful tool in standard geometric design. NURBS realizes the arbitrary shape of surface by adjusting its control points, knots weights and establishes a mapping relation between surface and parametric domain which is convenient for surface flattening and grid generation.

A *p*th-degree NURBS curve is shown in Fig.5 and is defined by [15]:

$$\mathrm{C}(u) = \frac{\sum_{i=0}^{n} N_{i,p}(u) \cdot \omega_i \cdot CP_i}{\sum_{i=0}^{n} N_{i,p}(u) \cdot \omega_i} \tag{1}$$

where $\{CP_i\}$ are the control points, $\{\omega_i\}$ are the weights, and $N_{i,p}(u)$ are the pth-degree B-spline basis functions which are:

$$N_{i,0}(u) = \begin{cases} 1 & if \ u_i \le u \le u_{i+1} \\ 0 & otherwise \end{cases}$$

$$N_{i,p}(u) = \frac{u - u_i}{u_{i+p} - u_i} N_{i,p-1}(u) + \frac{u_{i+p+1} - u}{u_{i+p+1} - u_{i+1}} N_{i+1,p-1}(u) \tag{2}$$

defined on the non-periodic and non-uniform knot vector:

$$U = \left\{ \underbrace{a, \dots, a}_{p+1}, u_{p+1}, \dots, u_{r-p-1}, \underbrace{b, \dots, b}_{p+1} \right\} \tag{3}$$

where $r = n + p + 1$.

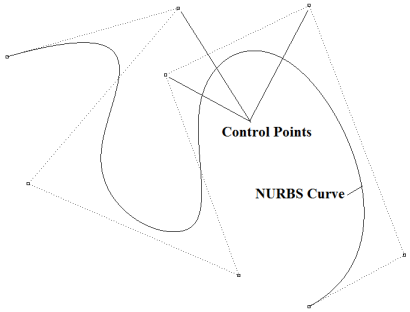

Figure 5: Relationship between a curve and its control points.

An NURBS surface (shown in Fig.6) of degree p in the u direction and degree q in the v direction is a bivariate vector-valued piecewise rational function with the following form [15]:

$$\mathrm{S}(u, v) = \frac{\sum_{i=0}^{n} \sum_{j=0}^{m} N_{i,p}(u) \cdot N_{j,q}(v) \cdot \omega_{i,j} \cdot CP_{i,j}}{\sum_{i=0}^{n} \sum_{j=0}^{m} N_{i,p}(u) \cdot N_{j,q}(v) \cdot \omega_{i,j}} \quad a \le u \le b, c \le v \le d \tag{4}$$

where $\{CP_{i,j}\}$ forms a bidirectional control net, $\{\omega_{i,j}\}$ are the weights, and $N_{i,p}(u)$, $N_{j,q}(v)$ are the non-rational B-spline basis functions defined on the knot vectors:

$$\begin{cases} U = \left\{ \underbrace{a, \dots, a}_{p+1}, u_{p+1}, \dots, u_{r-p-1}, \underbrace{b, \dots, b}_{p+1} \right\} \\ V = \left\{ \underbrace{c, \dots, c}_{q+1}, v_{q+1}, \dots, v_{s-q-1}, \underbrace{d, \dots, d}_{q+1} \right\} \end{cases} \tag{5}$$

where $r = n + p + 1$ and $s = m + q + 1$.

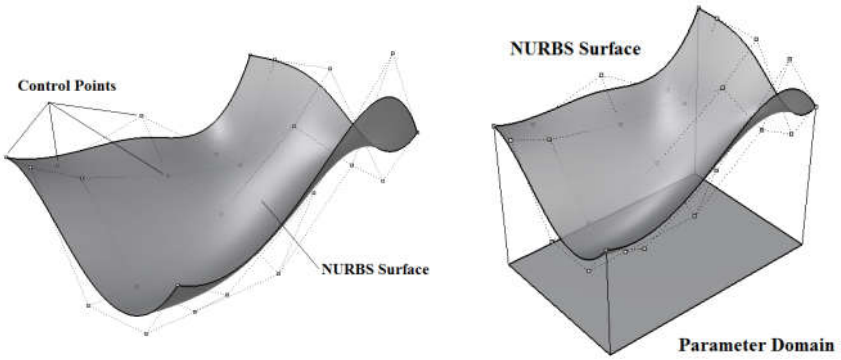

Figure 6: The relationship between a curved surface and its control points and mapping from parametric domain to the NURBS surface.

The curve mentioned above is defined in the three-dimensional space. However, in the current paper, the curves are always lying on the surface. It should be described by a two-time mapping rather than a single function, as shown in Fig.6. It is defined by an NURBS surface $\mathrm{S}(u, v)$ and a two-dimensional NURBS curve $\mathrm{C}(w)$ which lies on the parameter field of the surface. The value domain of the curve $\mathrm{C}(w)$, is in the definitional domain of the surface $\mathrm{S}(u, v)$. The pair of (u, v) is calculated from a parameter w by the function $\mathrm{C}(w)$. The three-dimensional coordinate is subsequently calculated from the pair of parameters (u, v) by the function $\mathrm{S}(u, v)$. It is obvious that all of the coordinates obtained by this two-time mapping method are exactly on the surface.

3 SURFACE FLATTENING

Surface flattening is a technique that transfers 3D surface into a plane surface, further operations can therefore be conducted on the plane surface which is less difficult compared to direct operations on 3D curved surface. Therefore, the surface flattening technique has been widely used in engineering practice, for example, to calculate and design blank shape in manufacture industry [16]. Surfaces are classified as developable and undevelopable surfaces according to the developability of a surface. Gaussian curvature is used to define developability of surface and the sufficient/necessary condition for a developable surface is that Gaussian curvature of surface is zero everywhere [17]. The surface flattening technique has been used in the design of membrane structures, Topping and Iványi [18] introduced a method to transform the 3D strips of membrane surface to planes for membrane cutting pattern generation based on the dynamic relaxation algorithm. In their method, the surface flattening process does not require the strip to be developable. At present, there are three methods of surface flattening including geometric flattening, mechanical flattening and combined geometric flattening and mechanical amendment [16, 19, 20]. This paper will use geometric flattening method to unfold surface based on the rule of identical area.

The geometric flattening method is applied to flatten surface based on the rule of equivalent area. A trimmed crescent shape surface is taken as example, as shown in Fig.7, which are the trimmed surface with complex boundaries and its complete surface, respectively.

Figure 7: Trimmed crescent shape surface with complex boundary and its complete surface.

3.1 Surface discretizing

The parametric domain of the free-form surface is divided into a number of segments in u and v direction on the basis of a relationship between surface adjacent boundary lengths. The parametric domain can be discretized into N×M grids corresponding to approximate equality or inequality of surface adjacent boundary lengths. Discrete free-form surface is therefore generated by mapping dividing points of the parametric domain onto the surface, as shown in Fig.8.

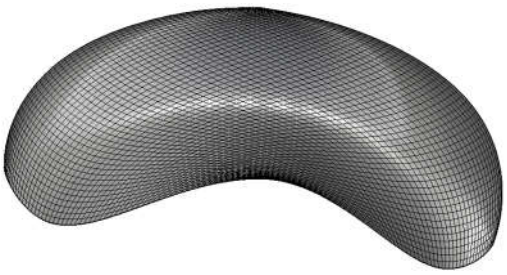

Figure 8: Surface discretizing.

3.2 Flattening of the central point and surrounding points

The central point of the surface mesh is then taken as the flattening center. The coordinates of unfolded plane points corresponding to the flattening center and its surrounding 8 points on the surface should be firstly determined, as shown in Fig.9.

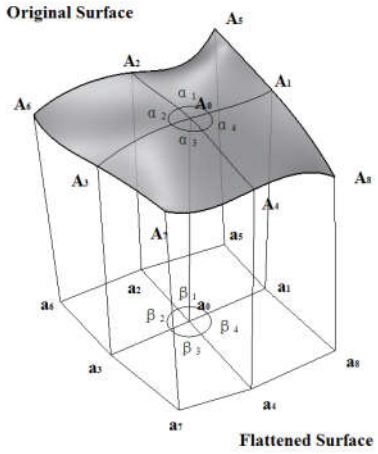

Figure 9: Flattening center and its surrounding points before and after flattening.

The corresponding point of the flattening center A_0 is point a_0 on the plane that is regarded as origin of the flattening plane. Suppose γ is added value of the summation of internal angles around the flattening center before and after flattening:

$$\gamma = 2\pi - (\alpha_1 + \alpha_2 + \alpha_3 + \alpha_4) \tag{6}$$

Value γ will be allocated to 4 regions so that the corresponding angles on the plane after flattening can be obtained. After the flattening:

$$\beta_i = \alpha_i + \gamma \times \alpha_i / \sum \alpha_i \tag{7}$$

Suppose u and v directions have the same rate of expansion that is called t before and after flattening, as the following equation:

$$t = \frac{|a_0a_1|}{|A_0A_1|} = \frac{|a_0a_2|}{|A_0A_2|} = \frac{|a_0a_3|}{|A_0A_3|} = \frac{|a_0a_4|}{|A_0A_4|} \tag{8}$$

According to the rule that the sum of triangles $\triangle a_0a_1a_2$, $\triangle a_0a_2a_3$, $\triangle a_0a_3a_4$, $\triangle a_0a_4a_1$ areas after flattening is equal to the sum of the corresponding triangle areas before flattening, value of t is obtained:

$$|A_0A_1||A_0A_2|\sin\alpha_1 + |A_0A_2||A_0A_3|\sin\alpha_2 + |A_0A_3||A_0A_4|\sin\alpha_3 + |A_0A_4||A_0A_1|\sin\alpha_4$$

$$= t^2(|A_0A_1||A_0A_2|\sin\beta_1 + |A_0A_2||A_0A_3|\sin\beta_2 + |A_0A_3||A_0A_4|\sin\beta_3 + |A_0A_4||A_0A_1|\sin\beta_4) \tag{9}$$

Substituting t into the formula (8), $|a_0a_1|$, $|a_0a_2|$, $|a_0a_3|$ and $|a_0a_4|$ are obtained. Combined with formula (7), the coordinates of points a_1, a_2, a_3, a_4 can therefore be achieved. Finally, according to the principle of identical area, the coordinates of points a_5, a_6, a_7, a_8 can be calculated. Taking a_5 as an example, suppose E_1, E_2, E_3 represent the area of triangle $\triangle A_1A_2A_5$, $\triangle A_0A_1A_5$, $\triangle A_0A_2A_5$ individually. Likewise, S_1, S_2, S_3 represent the area of corresponding triangle after flattening. If there are three points $P_1(x_1, y_1)$, $P_2(x_2, y_2)$, $P(x, y)$ to be in an anticlockwise arrangement on any plane. P_1, P_2 are fixed points and P is a moving point. The area of the triangle made up of these three points is as follows:

$$\varepsilon = \frac{1}{2}\begin{vmatrix} x_1 & y_1 & 1 \\ x_2 & y_2 & 1 \\ x & y & 1 \end{vmatrix} \tag{10}$$

Assume ΔS represents the summation of the squares of variation of the quadrilateral area before and after flattening:

$$\Delta S = \sum_{i=1}^{3}(S_i - E_i)^2 \tag{11}$$

In order to get the minimum value of ΔS, the following formula is applied:

$$\begin{cases} \frac{\partial \Delta S}{\partial x} = 0 \\ \frac{\partial \Delta S}{\partial y} = 0 \end{cases} \tag{12}$$

The x and y values which are the coordinates of point a_5 will then be obtained by solving the equations (7). Similarly, the coordinates of a_6, a_7, a_8 can be obtained in the same way.

3.3 Grids flattening of the whole regions

The entire surface is divided into four regions when the surface flattening center is determined, the regions will then be flattened in sequence. Following the flattening of A_0 and the surrounding 8 points, point A_2, which is on the right of point A_0 (Fig.9) is used as the center to flatten its surrounding points according to the principle of identical area. All grids will be flattened by repeating the above steps and the detailed flattening steps are shown in Fig.10.

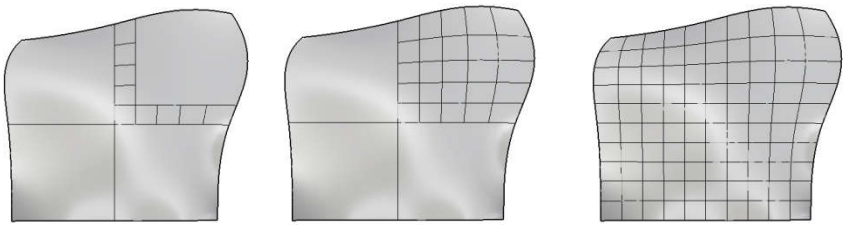

Figure 10: The steps of grids flattening: (a) Grid nodes of the first region flattening in a row (b) Grid nodes of the first region flattening and (c) Grid nodes of four regions flattening.

The discrete surface in Fig.8 is flattened based on above method. The flattening result is shown in Fig.11.

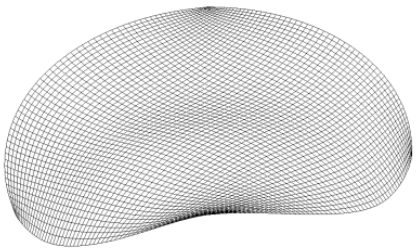

Figure 11: Rectangular lattices of the unfolded plane

It is worth noting that the method used here takes into account of a number of factors such as the shape of surface and relationship between surface adjacent boundary lengths when discretizing the surface. Geometric flattening method based on the principle of equivalent area can avoid cracks and overlaps during the surface flattening process. In addition, this method is easier to implement, therefore, has a preferable applicability.

4 GRID GENERATION BASED ON IMPROVED GUIDE-LINE METHOD

After the flattening of the free-form surface, the flattened rectangular lattices are fitted onto the 2D surface where grids are generated by employing the improved guide line method. The fitted 2D surface is shown in Fig.12.

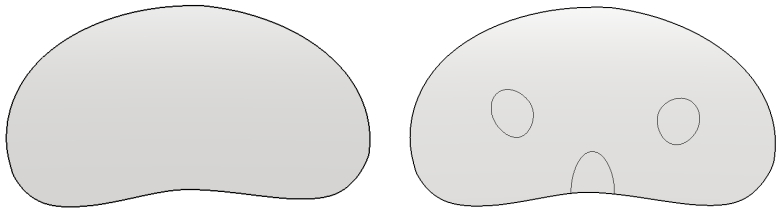

Figure 12: The fitted 2D surface and the trimming boundary on the flattened 2D surface.

The fitted 2D flattened surface share the same parametric field with the original 3D free-form surface. So, the original trimming boundary could be mapped to the 2D flattened surface as shown in Fig.12.

The guide line method to generate grids on free-form surface is in a way that a curve which is sketched on the surface by the architect determines the grid trend. The basic idea of grid generation is that the entire surface will be covered with multiple guide lines by advancing the predefined guide line which can manifest the designer's intuition. The fluency and regularity of the grid cells have been largely determined by the advanced guide lines, therefore, the guide line advancing technique is the key feature of grid generation [13]. The guide line method presented by Gao et al. [13] is improved in this paper which can generate grids on free-form surface with complex boundary conditions.

4.1 The guide line advancing

First the initial guide line should be sketched on the original surface by the designer, as shown in Fig.13. This guide line will directly be mapped to the flattened 2D surface, since the original surface and the flattened surface are in the same parametric field, as shown in Fig.13.

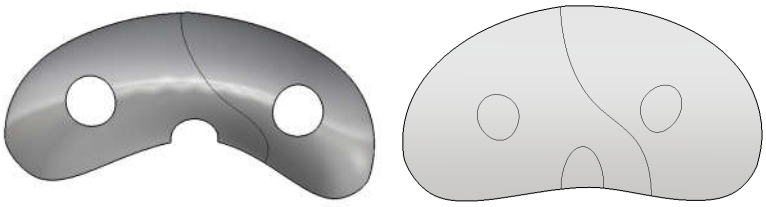

Figure 13: The initial guide line on the original surface and on flattened complete surface.

The new guide lines will be generated by advancing all the control points of the preceding guide line in a fixed distance in the same direction. The advancing distance is generally decided by the required member length (l) of the grid shell. Taking the NURBS surface in Fig.9 as an example and starting from the initially defined guide line (Fig.13), the resulted plane covered with guide lines is shown in Fig.14.

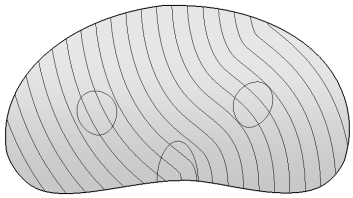

Figure 14: The flattened complete surface covered with guide lines.

4.2 The intersections between guide lines and boundaries

After the flattened 2D complete surface is covered with guide lines, the intersections between each guide line and the boundaries are calculated. This allows the guide lines to be trimmed. A special case is that the guide line is tangent to the boundary curve so the intersection point should be neglected. Suppose that the number of intersection points on each guide line starts from 1. If the 1st intersection is on the boundary, then the curves with even value of intersection number to odd intersection number (such as 2-3, 4-5) should be deleted, otherwise the curves from odd intersection number to even intersection number (such as 1-2, 3-4) should be deleted. The resulted of trimmed guide lines on the flattened surface is shown in Fig.15.

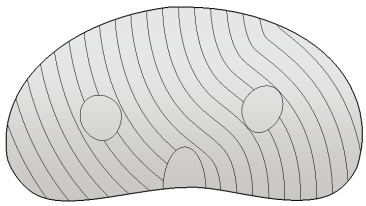

Figure 15: The trimmed guide lines on the flattened 2D surface.

4.3 Mapping the guide lines to original surface

Since the original surface share the same parametric field with the flattened 2D surface, the guide lines can therefore be mapped to the original surface directly.

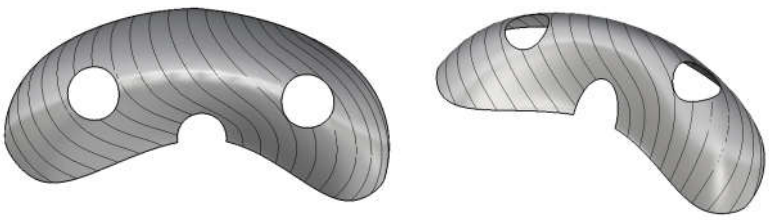

Figure 16: Guide lines on the original surface.

As shown in Fig.16, the guide lines on the surface are smooth and fluent. If guide lines of two directions are generated, the quadrilateral grids can be obtained. The final results of grids will be shown in the case studies.

5 GRID RELAXATIONS

The grid generated in previous method are generally fluent and with regular grid cells. However, a relaxation method may be needed to further smooth of the generated grids, as implemented by Williams [21] in the form design of the British Museum Great Court. The Particle-spring method has been successfully used by Kilian and Ochsendorf [22] at Massachusetts Institute of Technology, for form-finding of structural forms in pure compression or tension. In their method, axial springs connecting lumped masses were used to represent the physical behavior of a grid shell with truss members. The external gravity forces were then applied at the structural system while a final equilibrium of the structure was achieved. The method has been improved and adapted for the optimisation of generated grids by introducing a "pulling force", as shown in Fig.17 and this force prevents the particles from moving outside of the pre-defined surface. The particle-spring system serves as an excellent approximation for the grids generated and the equilibrium position of each mass on the surface is therefore achieved through an iterative process.

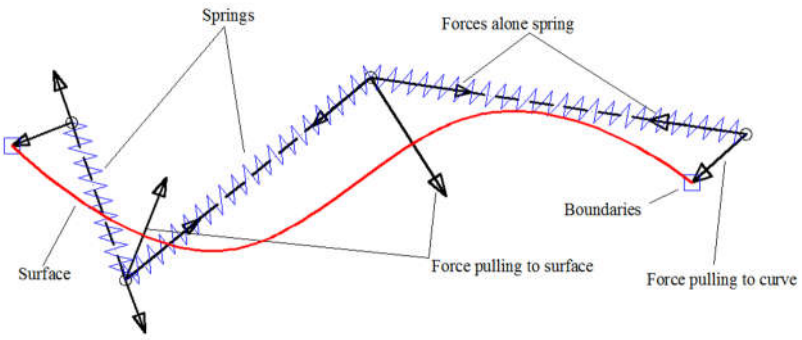

Figure 17: The equilibrium of the particle-spring system.

In the grids resulted from the surface flattening and guide line method, each node of the grids can be regarded as a particle and the members considered as springs in the particle-spring system. It is worth noting that the resulted grids are on the pre-defined surface. However, when the springs with different lengths are introduced with an initially expected equal rod length l, the forces in the particle-spring system will not be equilibrium. To prevent the particles in the particle-system from moving outside of the original surface, a constraining force pointing at the surface and the boundary curves are therefore introduced.

There are three types of forces in the particle-spring system, as shown in Fig.17. First, the force between two particles with a spring connected is introduced. The second force stems from a particle which is fixed, such particles are generally defined on the boundries of the resulted grids. Finally, forces are defined to preventing the particles from moving outside the surface and the boundary curves.

Each particle is assumed to have a constant lumped mass m. In the meantime, each rod is taken as a linear elastic spring with a constant free length l, and a constant axial stiffness k_{spring}. The lumped mass m can be set as unit. The stiffness k_{spring} will therefore affect the convergence speed. The stiffness is set as a larger value during the initial iterations to

accelerate the convergence, and gradually reduced to achieve stable results. Each spring loads with a force along its length as:

$$f = (l_{cu} - l) \cdot k_{spring} \tag{13}$$

where the l_{cu} is the deformed length of the spring. Each particle i will be subjected to unbalanced internal forces from its connecting springs as:

$$F_{spring,i} = \sum_{(i,j)\in\{S\}} f_{i,j} \tag{14}$$

in which the {S} is a set containing all springs.

For the particles on the boundaries, a force $F_{curve,i}$ with a normal direction through itself will be used to pull the particles back to the boundary curve.

$$F_{curve,i} = k_{curve} \cdot d_{curve,i}^{e_1} \tag{15}$$

in which k_{curve} is a coefficient, larger values of k_{curve} indicate a stronger constraint on the particles. $d_{curve,i}$ is the distance between the particle and the boundary curve which can be calculated by a computational geometry method presented by Piegl [15]. e_1 is an exponent and a penalty parameter of the distance. A larger factor of $e1$ means the particle further from the boundary curves will be subjected to more constraints to accelerate the convergence while the particles closer to the boundary curves will be subjected to less constraints to avoid oscillation.

For the other particles, a force $F_{surface,i}$ with a fictional force will be used to keep the particles sliding on the surface:

$$F_{surface,i} = k_{surface} \cdot d_{surface,i}^{e_2} \tag{16}$$

where $k_{surface}$ is a coefficient similar to k_{curve}. $d_{surface,i}$ is the distance between the particle and the surface. e_2 is the exponent parameter, which is similar to e_1.

The resultant force of each particle can be calculated by:

$$F_i = F_{spring,i} + \begin{cases} F_{curve,i} & for\ particles\ on\ boundary\ curves \\ F_{surface,i} & for\ other\ particles \end{cases} \tag{17}$$

Then motion equations of all particles with viscous damping are shown as:

$$a_{t,i} = \frac{F_{t,i} - c \cdot v_{t,i}}{m} \tag{18}$$

$$v_{t+1,i} = v_{t,i} + a_{t,i} \cdot \triangle t \tag{19}$$

$$d_{t+1,i} = d_{t,i} + \frac{1}{2}\left(v_{t+1,i} + v_{t,i}\right) \triangle t \tag{20}$$

These formulas are the classical kinematic equations of particles in a viscous damping environment. $F_{t,i}$, $a_{t,i}$, $v_{t,i}$ and $d_{t,i}$ are the force, acceleration, velocity and position for the mass particle i of time t, respectively. c is the viscous damping coefficient. $\triangle t$ is the length of the discrete time step.

An iterative process to solve the equations of motion of each particle has been presented in dynamic relaxation method in order to achieve static equilibrium. Such technique has traditionally been widely applied to the form-finding of cable-net and membrane structures [18, 21, 23, 24]. A discussion on the effects of parameters on convergence of the solver has been discussed in the dynamic relaxation method [25, 26]

6 CASE STUDIES

The steel and glass roof of the British Museum Great Court covers a rectangular area which is 70 m in width and 100 m in length. The Reading Room, which has a cylindrical shape with a diameter of 44 m, is located slightly off the centre of the court. The shape of the roof can be expressed as a mathematical function and more information is provided by William [21]. The original trimmed surface is shown in Fig. 18.

Figure 18: Original trimmed surface of British Museum Great Court Roof.

The complete surface was obtained as shown in Fig. 19 using the analytical equations [21]. The original complete surface had a sharp corner at the center of the surface, is therefore not suitable for surface flattening and the following grid generation.

(a) Right view

(b)Perspective view

Figure 19: Complete surface of British Museum Great Court Roof.

A surface reconstruction procedure was therefore employed to the surface. The control points at the center of the original surface shown in Fig.19 were lifted by a distance. Then the surface was reconstructed with some of the control points replaced while the weights and knots were kept the same, as shown in Fig.20. The reconstructed surface was discretized, flattened and fitted by employing the procedures presented above and the flattened surface is shown in Fig. 20.

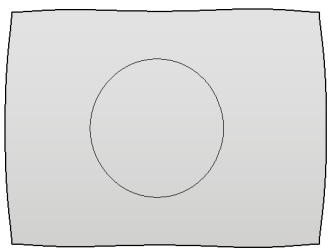

Figure 20: Reconstructed complete surface and fitting the trimming boundary to the flattened and reconstructed surface.

Since the surface is symmetrical along its horizontal axis, the diagonals with different shapes were chosen as the initial guide lines. Crossing guide lines were used to generate the quadrilateral mesh on the flattened surface, and the generated grids were then mapped to the surface. It is shown that the trends of the generated grids vary with the initial guide lines definition. The grids were generally fluent even without any grid relaxation process.

Initial guide lines with 3 different directions were taken as examples to show the grid generation process. The initially defined guide lines in Case 1 are assumed to be along the diagonals of the surface (Fig.21) and the results are shown in Fig. 22-27. Fig. 22 shows the result from 2 different directions of initially defined guide lines without any post process. The resulted grids are fluent whereas there were several short rods at the boundaries of the surface. The vertices which are close to each other at the boundaries were merged given a certain threshold. The grids shown in Fig.22 are then relaxed and the results are shown in Fig. 23. Compared to the results in Fig.22, less short rods along their boundary curves are observed in the results presented in Fig.23. Fig.24 shows the decreased variance of member length with regard to the iterations of grid relaxation, the relaxed grids are shown to be more fluent.

If the diagonals of each quadrilateral grid cell were generated, as shown in Fig. 25, the triangular grids were obtained. Since the rods were not very smooth with kinks at the diagonals of the grids, the grid relaxation procedure was employed and the results are shown in Fig. 26. It can be shown that the resulted grids are more fluent when the grid relaxation procedure is used. Fig.27 shows the decreased variance of member length with regard to the iterations of grid relaxation. Compared to the results in Fig.25, the kinks presented at the diagonals have been eliminated after the grid relaxation process.

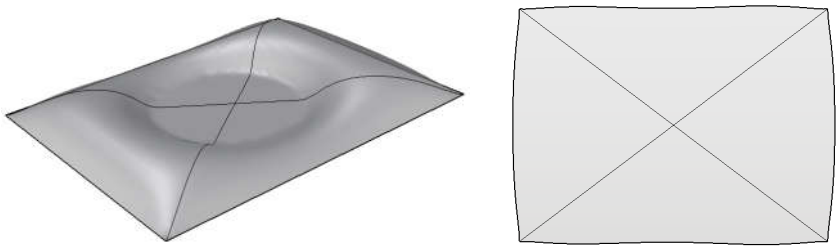

Figure 21: Case 1: initially defined guide lines on (a) reconstructed complete surface and (b) flattened surface.

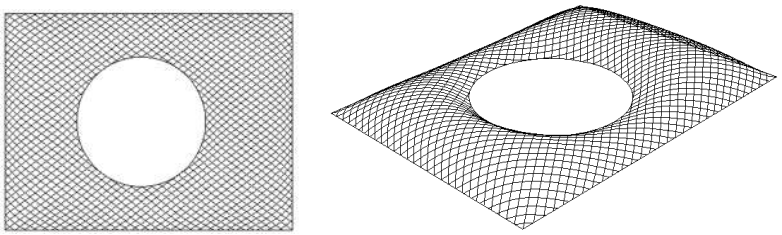

Figure 22: Quadrilateral grids of case 1.

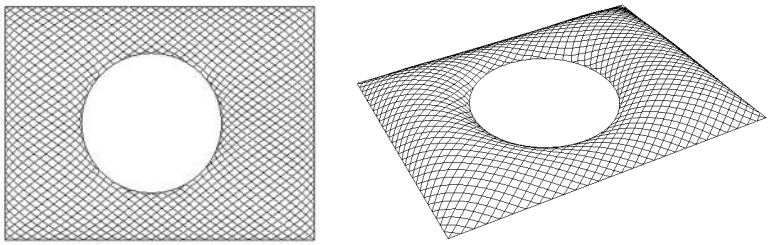

Figure 23: Relaxed quadrilateral grids of case 1.

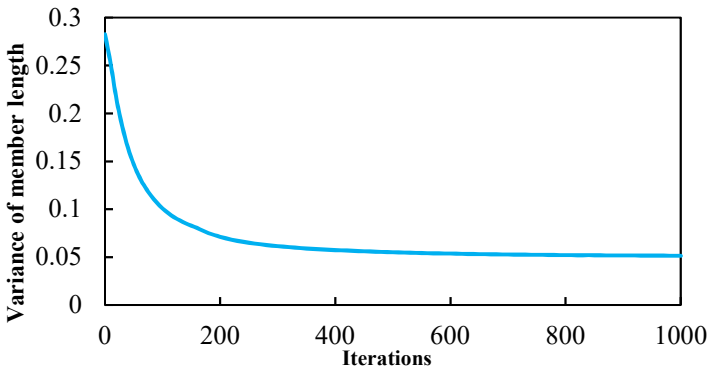

Figure 24: Change of member length to the iterations for the quadrilateral grid.

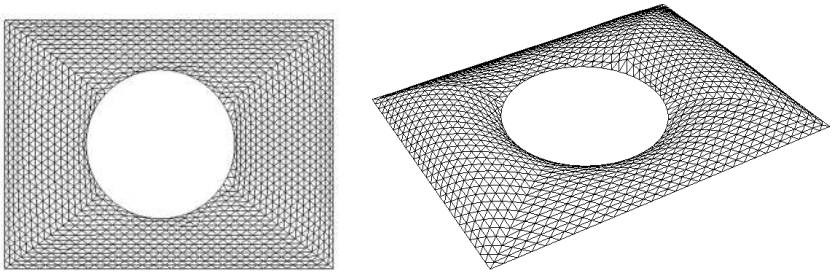

Figure 25: Triangular grids of case 1.

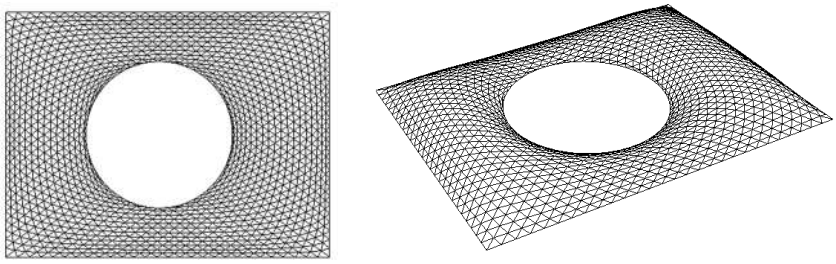

Figure 26: Relaxed Triangular grids of case 1.

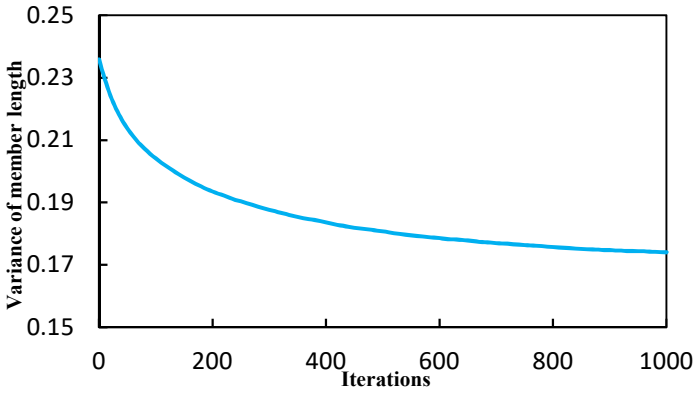

Figure 27: Variance of member length to the iterations for the triangular grid.

Case 2 presented the results from 2 different initially defined guide lines in Fig.28 and the results are compared to those from case 1. The generated grids without any post process were shown as Fig. 29. The relaxed quadrilateral grids were shown in Fig. 30. The triangular grids were generated by connecting diagonals of each quadrilateral cell and are shown in Fig. 31while the relaxed triangular grids were shown in Fig. 32.

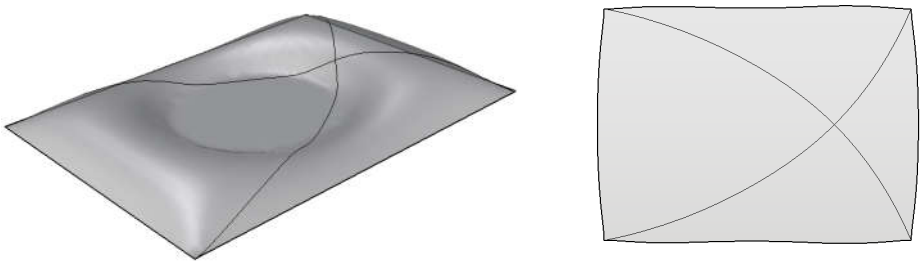

Figure 28: Case 2: initially sketched guide lines on (a) reconstructed complete surface and (b) flattened surface.

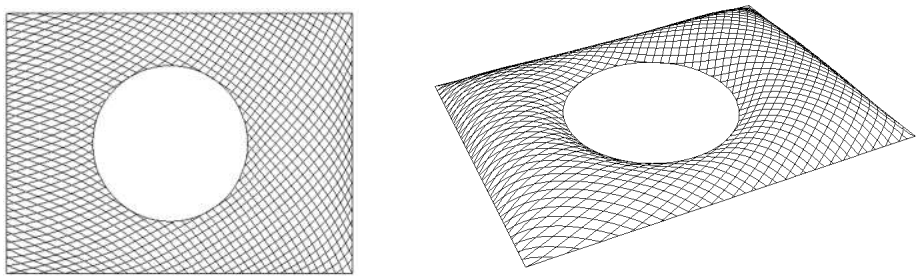

Figure 29: Quadrilateral grids of case 2.

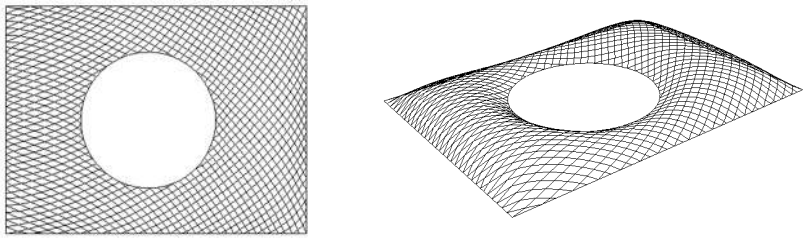

Figure 30: Relaxed quadrilateral grids of case 2.

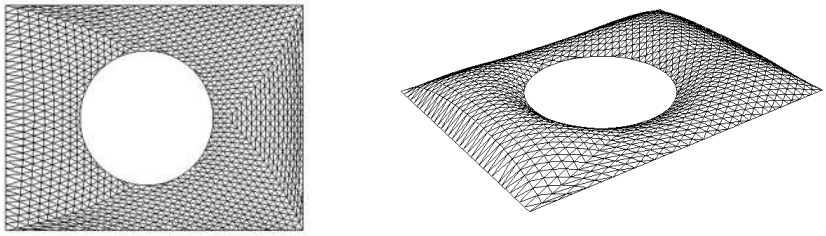

Figure 31: Triangular grids of case 2.

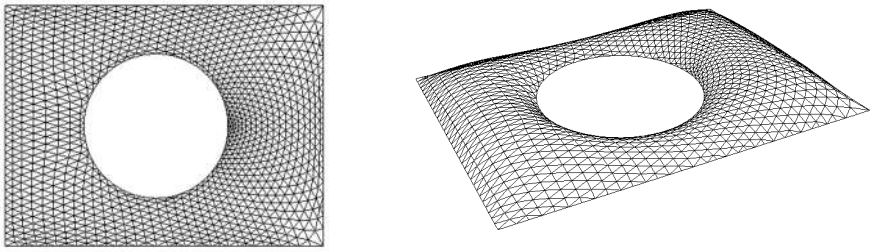

Figure 32: Relaxed Triangular grids of case 2.

Case 3 is the third example with the intersection of initially defined guidelines on the left side of the circle (Fig.33). The results were shown as Fig. 34 – 37. The guide lines to generate the quadrilateral girds without any post process were shown as Fig. 34. The relaxed quadrilateral grids were shown in Fig. 35. The triangular grids by connecting diagonals in each quadrilateral grid cell were shown in Fig. 36 while the relaxed triangular grid pattern was shown in Fig. 37.

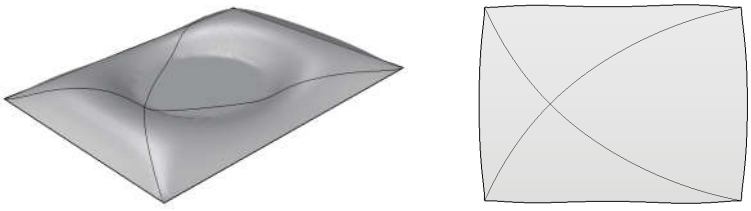

Figure 33: Case 3: initially sketched guide lines on (a) reconstructed complete surface and (b) flattened surface.

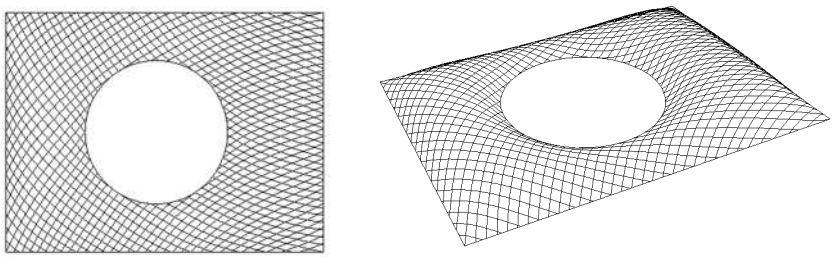

Figure 34: Quadrilateral grids of case 3.

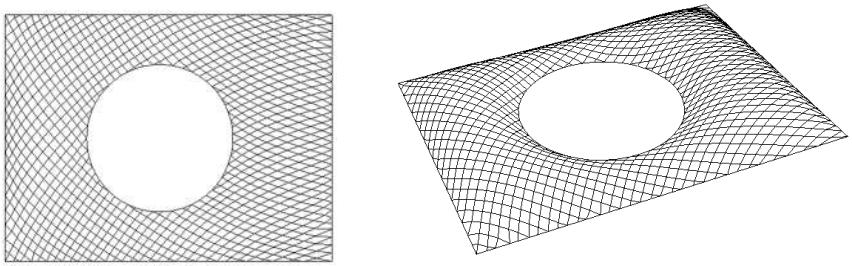

Figure 35: Relaxed quadrilateral grids of case 3.

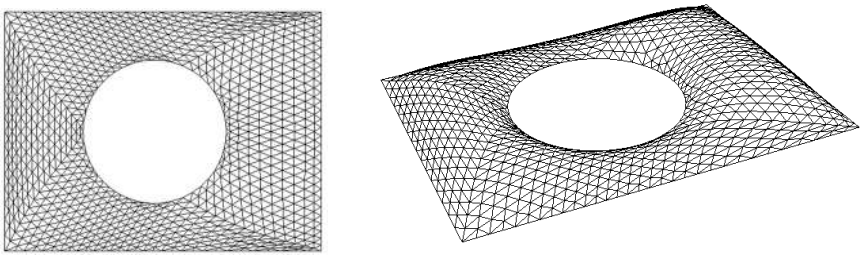

Figure 36: Triangular grids of case 3.

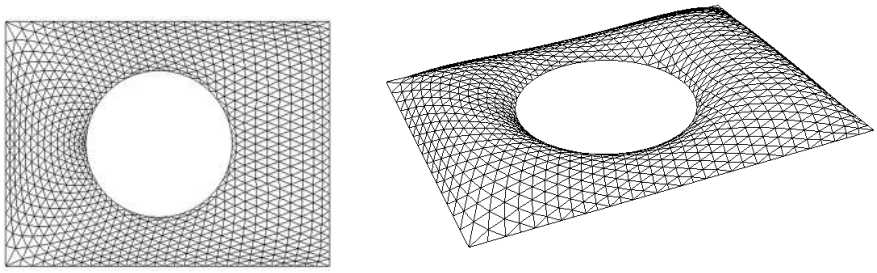

Figure 37: Relaxed triangular grids of case 3.

It is also shown in these 3 cases that by defining different guide lines on the surface, various solutions can be obtained. The initially defined guide lines can therefore set the tone of the grid and reveals the intent of the designer.

7 SOFTWARE DEVELOPMENT

The grid generation and the spring-mass method was programmed into software 'ZD-Mesher'[13], specifically developed by the authors for the purpose of free-form grid generation. The software was developed for a Microsoft Windows operating system with C++. The GUI framework was based on MFC (Microsoft Foundation Classes). A screen shot of the GUI is shown in Fig. 38.

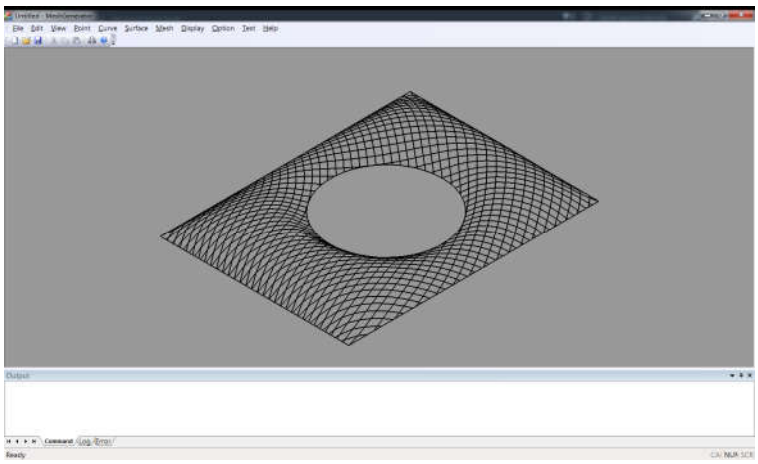

Figure 38: GUI of the ZD-Mesher software

Apart from implementing the algorithms for grid generation, the software provides essential visualization and data exchange functions. It also provides commands assisting with sketching a curve on the surface, dividing a curve into segments by number or by length and merging several curve sections into a single curve for further operations. The software is also able to exchange data with other commercial software packages as part of an integrated design process. Data formats such as IGES, STEP, BREP, and STL are supported. As a result, the software can communicate with almost any industrial CAD/CAM product. In addition, the software can export the geometric data to commercially available structural analysis packages such as ANSYS [27], ABAQUS [28] and SAP2000 [29].

8 CONCLUSIONS

A grid generation and relaxation technique on free-form surface with complex boundary for grid shell structure design is put forward, based on the surface flattening technique and the improved guide line method. The parametric domain of the complete NURBS surface was firstly divided into a number of parts and a discrete free-form surface was formed by mapping dividing points onto surface. The free-form surface was then flattened based on the principle of identical area. Accordingly, the flattened rectangular lattices were fitted into the 2D surface where grids were formed by employing the guide line method. Subsequently, the intersections of guide lines and the complex boundary were obtained then the guide lines were therefore divided equally to obtain grids by connecting dividing points while the grids outside the design domain were deleted. Finally, the 2D grids were mapped onto the 3D surface to achieve the grid on free-form surface with complex boundary for design use. A spring-mass method was also employed to further improve the smoothness of the resulted grids. The grids generated by this method on the complex surface not only met the requirements of regular shape and fluent lines, embodied the trends of grids and the connotation of architecture, but

also had high quality of grids around the inner boundary. The method was programmed and added into software developed by the team of authors in order to facilitate the grid generation process.

ACKNOWLEDGEMENTS

This research was sponsored by the National Natural Science Foundation of China under Grant 51378457, Grant 51678521 and Grant 51778558 and by the Natural Science Foundation of Zhejiang Province under Grant LY15E080017. The project is also supported by the Foundation of Zhejiang Provincial Key Laboratory of Space Structures, Grant 21705. The financial supports are gratefully acknowledged by the authors.

REFERENCES

[1] Malek S. and Williams C.J., "Reflections on the Structure, Mathematics and Aesthetics of Shell Structures", *Nexus Network Journal*, **19**, 555-563, 2017.

[2] Shilin D., "Development and expectation of spatial structures in China", *Journal of Building Structures,* **31(6)**, 38-51, 2010.

[3] Kang W., Chen Z., Lam H-F. and Zuo C., "Analysis and design of the general and outmost-ring stiffened suspen-dome structures", *Engineering Structures*, **25**, 1685-1695, 2003.

[4] Cui C.Y. and Jiang B.S., "A morphogenesis method for shape optimization of framed structures subject to spatial constraints", *Engineering Structures*, **77**, 109-118, 2014.

[5] Aubry R., Houzeaux G. and Vazquez M., "A surface remeshing approach", *International Journal for Numerical Methods in Engineering*, **85**, 1475-1498, 2011.

[6] Hannaby S.A.. "A Mapping Method for Mesh Generation", *Computers & Mathematics with Applications*, **16**, 727-735, 1988.

[7] Muylle J., Iványi P. and Topping B., "A new point creation scheme for uniform Delaunay triangulation", *Engineering Computation*, **19**, 707-735, 2002.

[8] Liu Y., Xing H.L. and Guan Z.Q., "An indirect approach for automatic generation of quadrilateral meshes with arbitrary line constraints", *International Journal for Numerical Methods in Engineering*, **87**, 906-922, 2011.

[9] Popov EV., "Geometric approach to chebyshev net generation along an arbitrary surface represented by nurbs", International conference on computer graphics and vision, 2002.

[10] Lefevre B., Douthe C. and Baverel O., "Buckling of elastic gridshells", *Journal of the International Association of Shell and Spatial Structures*, **56(3)**, 153-171, 2015.

[11] Shepherd P. and Richens P., "The case for subdivision surfaces in building design", *Journal of the International Association for Shell and Spatial Structures*, **53**, 237-245, 2012.

[12] Douthe C., Mesnil R., Orts H. and Baverel O., "Isoradial meshes: Covering elastic gridshells with planar facets", *Automation in Construction*, **83**, 222-236, 2017.

[13] Gao B., Li T., Ma T., Ye J., Becque J. and Hajirasouliha I., "A practical grid generation procedure for the design of free-form structures", *Computers & Structures*, **196**, 292-310, 2017.

[14] Gao B., Hao C., Li T. and Ye J., "Grid generation on free-form surface using guide line advancing and surface flattening method", *Advances in Engineering Software*, **110**: 98-109, 2017.

[15] Piegl L. and Tiller W., *The NURBS book*: Springer Science & Business Media, 2012.

[16] McCartney J., Hinds B. and Chong K., "Pattern flattening for orthotropic materials", *Computer-Aided Design*, **37**, 631-644, 2005.

[17] Banchoff T.F. and Lovett S.T., *Differential geometry of curves and surfaces*, CRC Press, 2015.

[18] Topping B.H. and Iványi P., *Computer aided design of cable membrane structures*, Saxe-Coburg Publications, 2008.

[19] Li J., Zhang D., Lu G., Peng Y., Wen X. and Sakaguti Y., "Flattening triangulated surfaces using a mass-spring model", *The International Journal of Advanced Manufacturing Technology*, **25**, 108-117, 2005.

[20] Wang C.C. and Tang K., "Woven model based geometric design of elastic medical braces", *Computer-Aided Design*, **39**, 69-79, 2007.

[21] Williams C.J., The analytic and numerical definition of the geometry of the British Museum Great Court Roof. In: Mathematics & design, Deakin University, 434-440, 2001.

[22] Kilian A. and Ochsendorf J., "Particle-spring systems for structural form finding", *Journal of the International Association for Shell and Spatial Structures*, **46**, 2005.

[23] Adriaenssens S., Ney L., Bodarwe E. and Williams C., "Finding the form of an irregular meshed steel and glass shell based on construction constraints", *Journal of Architectural Engineering*, **18**, 206-213, 2012.

[24] Richardson J.N., Adriaenssens S., Coelho R.F. and Bouillard P., "Coupled form-finding and grid optimization approach for single layer grid shells", *Engineering Structures*, **52**, 230-239, 2013.

[25] Topping B. and Khan A., "Parallel computation schemes for dynamic relaxation", *Engineering Computation*, **11**, 513-548, 1994.

[26] Barnes M., Form finding and analysis of tension space structures by dynamic relaxation, PhD thesis, City University London, 1977.

[27] ANSYS. User's Guide, Release 14.5, Ansys Inc, Canonsburg, 2012.

[28] ABAQUS 6.13, Analysis User's Guide, Dassault Systems, 2013.

[29] Berkeley C., Computer program SAP2000 V14, Computers and Structures Inc, Berkeley, California, 2011.